ISOTOPE SHIFT IN THE NEON GROUND-STATE BY EXTREME-ULTRAVIOLET LASER SPECTROSCOPY AT 74 NM

Eikema, K.S.E.; Ubachs, W.M.G.; Hogervorst, W.

published in
Physical Review A. Atomic, Molecular and Optical Physics
1994

DOI (link to publisher)
10.1103/PhysRevA.49.803

document version
Publisher's PDF, also known as Version of record

Isotope shift in the neon ground state by extreme-ultraviolet laser spectroscopy at 74 nm

K. S. E. Eikema, W. Ubachs, and W. Hogervorst
Department of Physics and Astronomy, Laser Centre Vrije Universiteit, De Boelelaan 1081, 1081 HV Amsterdam, The Netherlands
(Received 8 September 1993)

Narrow-band extreme-ultraviolet (xuv) radiation in the range 73.5–75.5 nm has been produced in Xe by generating the third harmonic of light from a frequency-doubled, pulsed blue-dye laser. In a one-xuv-photon plus one-uv-photon ionization process both $2p^6$-$2p^5 3s[\frac{3}{2}]_1$ and $2p^6$-$2p^5 3s'[\frac{1}{2}]_1$ transitions in ^{20}Ne and ^{22}Ne were observed. Frequencies were calibrated using a tellurium absorption spectrum of the fundamental blue light. Frequencies of 134 459.33(5) cm^{-1} for the $2p^6$-$2p^5 3s[\frac{3}{2}]_1$ and 135 888.73(5) cm^{-1} for the $2p^6$-$2p^5 3s'[\frac{1}{2}]_1$ transition in ^{20}Ne are obtained. In both transitions the isotope shift (^{20}Ne-^{22}Ne) was measured. The values are $-0.014(3)$ cm^{-1} and $+0.003(3)$ cm^{-1}, respectively. Combined with existing values for the $3s[\frac{3}{2}]_1$ and $3s'[\frac{1}{2}]_1$ level shifts, a value for the ground-state specific mass shift of 9.54(15) GHz is deduced, in good agreement with a theoretical value of 10.1 GHz.

PACS number(s): 32.30.−r, 32.80.Rm, 42.65.Ky

I. INTRODUCTION

Isotope shifts in atomic transition frequencies and level energies provide valuable insight into atomic as well as nuclear structure. These shifts are due to differences in nuclear mass (mass shift) and nuclear volume or charge distribution (field shift). The latter shift may be neglected for light elements such as Ne [1]. The mass shift consists of two parts, the normal mass shift (NMS, or Bohr shift) and the specific mass shift (SMS). Both terms result from the separation of the center-of-mass motion from the internal motion. The NMS is easy to evaluate and can be calculated by the replacement of the electron mass in the Hamiltonian by the reduced mass. In the SMS the correlation in the momenta of the electrons has to be considered [2]. Calculation of the SMS then requires knowledge of accurate wave functions [3]. In He, *ab initio* calculations to a high degree of precision are now possible, and excellent agreement with experiment is achieved [4]. For heavier elements such as Ne, however, wave functions are less well known. In most of the early work, results of Hartree-Fock calculations, in which higher-order relativistic effects are neglected, were reported. Reasonable, although not very accurate, values for the SMS could be estimated (see, e.g., [5]). Theoretical results from many-body perturbation calculations have become available recently for Ne. Ahmad [6], e.g., examined the SMS in $3s$-$3p$ transitions, whereas Hörbäck *et al.* [7] and Veseth [3] calculated the ground-state SMS.

Most experimental data concern shifts of the even isotopes ^{20}Ne-^{22}Ne. The low ^{21}Ne natural abundance (0.25% versus 90% ^{20}Ne and 9% ^{22}Ne) hampers the measurement of odd-even values. Early experimental work on Ne with a discharge lamp was performed by Ritchl and Schober [8,9]. They deduced the shift for many levels, up to the $10s$ state for which the shift was assumed to be zero. Their accuracy for the transition shifts was 3×10^{-3} cm^{-1}. The ground state of Ne was not studied in this work. The shifts in all transitions from the $3s$ to the $3p$ configurations were measured by Odintsov [10] with an accuracy of $\sim10^{-4}$ cm^{-1}. Konz, Kraft, and Rubahn [11] obtained a two-fold improved accuracy for the same transitions using laser spectroscopy, starting from the $3s$ $J=0$ and $J=2$ metastable states. Giacobino, Biriaben, and de Clercq [1] measured the shifts in two-photon transitions from the same two metastable states to the $4d$ and $5s$ configurations. Their accuracy of ~3 MHz revealed $J=1$ states to have an isotope shift that differs from states with $J\neq1$. Also, a dependence on core angular momentum was observed, in agreement with theoretical predictions. In addition, Salour [12] also used two-photon spectroscopy to measure the isotope shift in three transitions from the $2p^5 3s[\frac{3}{2}]_2$ state to the $7d$ configuration.

The only isotope-shift measurement involving the $2p^6$ ground state was, as far as we know, performed by Westerveld and van Eck [13]. They measured the self-absorption difference between pure ^{20}Ne and a 50%–50% ^{20}Ne-^{22}Ne mixture in the transition from the $2p^6$ ground state to the $3s[\frac{3}{2}]_1$ (74.4 nm), $4s[\frac{3}{2}]_1$ (63.0 nm), and $4s'[\frac{1}{2}]_1$ (62.7 nm) excited states using a discharge lamp. Combining their results with those of Ritchl and Schober [8], they could deduce a shift of 2 ± 3 GHz for the ground state. This resulted in a SMS of the ground state of 11 ± 3 GHz, in agreement with the theoretical value of 10.1 GHz calculated by Veseth [3].

The three-orders-of-magnitude difference in accuracy of data for transitions between excited states (~3 MHz) and for transitions involving the ground state (3 GHz) can be attributed to the problem in generating narrow-band short-wavelength (<75 nm) radiation. However, considerable progress in the production of narrow-band extreme-ultraviolet (xuv) radiation below 100 nm has been made using nonlinear up-conversion techniques. Coherent radiation down to 15 nm has been generated [14]. In most experiments high-peak-power picosecond pulsed lasers are used with the disadvantage of a large bandwidth. Accurate, sub-wave-number spectroscopy requires the use of tunable nanosecond lasers. Until recently, the shortest wavelength generated with ns lasers was

~70 nm [15–17]. In a recent experiment we successfully produced tunable 58.4-nm radiation by fifth-harmonic conversion and excited the $1\,^1S$-$2\,^1P$ transition of He [18].

In the present investigation, isotope shifts in Ne transitions from the ground state to the $3s[\frac{3}{2}]_1$ and $3s'[\frac{1}{2}]_1$ levels are measured with ~74-nm radiation which is produced by third-harmonic generation in Xe using a frequency-doubled blue-dye laser. An advantage of frequency tripling over, e.g., 2+1 resonant frequency mixing is the possibility to calibrate the fundamental frequency directly against the spectrum of molecular tellurium.

II. EXPERIMENTAL SETUP

In the setup shown in Fig. 1 a frequency-doubled blue-dye laser (Quanta Ray Model PDL3, Coumarine 450), pumped by the third harmonic of an injection-seeded Nd:YAG (where YAG denotes yttrium aluminum garnet) laser (Quanta Ray GCR4) is used. The uv light is generated in a crystal of β-barium borate (BBO), separated from the fundamental light by dichroic mirrors and focused with a lens in a pulsed Xe jet (Fig. 1). The two-photon resonance $6p'[\frac{1}{2},0]_1$ in Xe strongly enhances the third-harmonic-generation process as shown in Fig. 2, for both high- and low-density gas pulses. This resonance also easily induces optical breakdown in the nonlinear medium, at the uv power levels of 6–7 mJ used. Even at moderate uv intensity, for example, multiphoton transitions and the optical Kerr effect result in saturation of the xuv yield. To limit the intensity in the focus as well as to have an extended focal volume, a lens with a rather large focal length of 35 cm is used. This also results in a sufficiently high uv power density in the detection zone, thus facilitating the one-xuv-photon plus one-uv-photon ionization process. All measurements were performed using a "high" Xe density in the gas pulse [Fig. 2(a)]. In a separate vacuum chamber a pulsed solenoid valve produces a skimmed, sub-Doppler Ne beam. The 5-cm-distance between the nozzle and the 2-mm-diam skimmer reduces the divergence of the atomic beam to ~25 mrad; the xuv beam has a similar divergence. The spatially and temporally overlapping xuv and uv beams intersect the Ne beam at right angles in a third, differentially pumped excitation chamber. Diffusion pumps in combination with liquid-nitrogen baffles are used for the nozzle chambers; the excitation chamber is pumped with a turbomolecular pump. The intensity of the atomic beam was adjusted to give an interaction-zone pressure of $\sim 3\times10^{-7}$ mbar. Higher Ne-beam intensities, or shorter skimmer-nozzle distances, introduce asymmetric line profiles, severe line shifts, and broadening, especially for the strong $2p^6$-$2p^5 3s'[\frac{1}{2}]_1$ transition. These effects are probably due to the high-xuv-absorption cross section of Ne [19].

The xuv-induced excitations were detected by subsequent photoionization of the atom using the intense uv radiation. Ions are extracted by a small electric field of 30 V/cm and, after passing a 20-cm time-of-flight mass selector, detected with an electron multiplier. Two box-

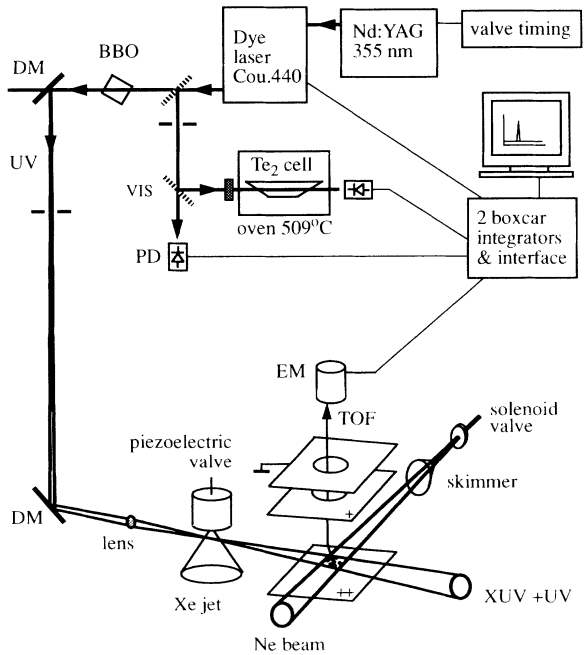

FIG. 1. Schematic of the experimental setup for xuv laser spectroscopy: DM, dichroic mirror; EM, electron multiplier; TOF, time of flight; VIS, visible light; PD, photodiode; and BBO, β-barium borate crystal.

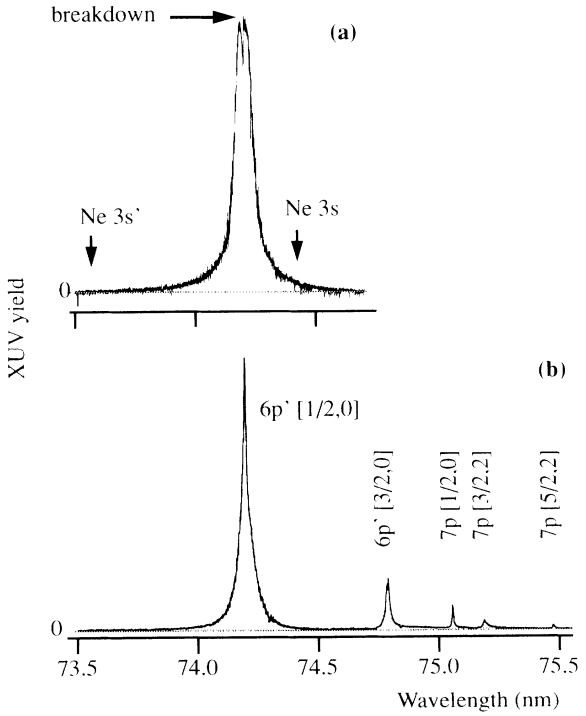

FIG. 2. Relative xuv yield using (a) high- and (b) low-density xenon gas pulses, measured by direct photoionization of C_3H_6. The two-photon resonances in xenon are indicated by their assignment; the arrows show the position of the $3s'[\frac{1}{2}]_1$ and $3s[\frac{3}{2}]_1$ neon resonances. Incident uv power is 6–7 mJ in 4 ns; the focal length of the lens used is 35 cm.

car integrators were used to measure signals of the ^{20}Ne and ^{22}Ne isotopes simultaneously, thus minimizing relative frequency error. The limited mass-resolving power of the time-of-flight detector prevented ^{21}Ne from being measured independently from the 300-times-stronger ^{20}Ne signal. Therefore, only ^{20}Ne and ^{22}Ne were measured. The neon resonance lines were fitted to Voigt profiles.

For calibration purposes, an absorption spectrum of Te_2 was recorded simultaneously (the xuv wavelength is exactly one-sixth of the blue-dye laser wavelength). A 7-cm quartz cell at 509(5) °C was used for this purpose. To avoid possible laser-induced frequency shifts, the incident power was reduced to 20 nJ. The absorption spectrum was normalized for dye-laser intensity, and the Te_2 line profiles were fitted to Gaussians.

The original PDL3 dye-laser stepper-motor drive was modified with a 1:13 gearing wheel to improve the regularity in the scan, and to reduce the average step size to 8.33×10^{-3} cm^{-1} for the Te_2 calibrated spectra and 1.66×10^{-3} cm^{-1} for the isotope-shift measurements. Although step-to-step irregularities could be eliminated in this way, the scan of the dye laser also showed oscillations [amplitude $\pm(2-3)\%$] with a typical period of a few wave numbers. Because of the limited number of Te_2 lines that could be resolved, these oscillations are difficult to compensate. In a similar experiment on He [18], it was shown that, with the help of an appropriate étalon to interpolate between the reference lines, the error introduced in the absolute calibration by nonlinear scanning can be reduced to 0.02 cm^{-1} or less. A similar, "blue" étalon was not available for the Ne experiment, so absolute calibration was obtained by a linear least-squares fit through as many reference lines as possible (see Figs. 3 and 4; Te_2 lines are marked by their number according to Ref. [20]). For the isotope-shift measurements, the dye-laser scan was sufficiently regular, because here only frequency differences are important. In this case it was not necessary to record a Te_2 calibration spectrum. All data points were obtained by averaging over 20 laser shots to reduce the influence of shot-to-shot power fluctuations.

III. RESULTS AND DISCUSSION

In the upper part of Figs. 3 and 4, the $2p^6$-$2p^5 3s[\frac{3}{2}]_1$ and the $2p^6$-$2p^5 3s'[\frac{1}{2}]_1$ transitions of ^{20}Ne at 134 459.33(5) and 135 888.73(5) cm^{-1}, respectively, are shown. Both frequencies are in agreement with the classical spectroscopic values of 134 459.29(4) and 135 888.72(4) cm^{-1} obtained by Kaufman and

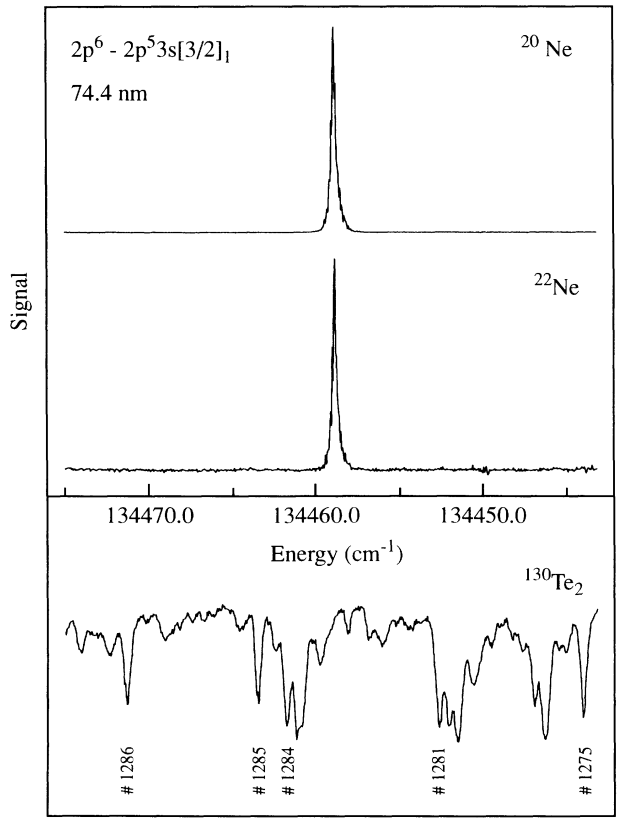

FIG. 3. The $2p^6$-$2p^5 3s[\frac{3}{2}]_1$ transition in ^{20}Ne and ^{22}Ne at 74.4 nm with the calibration spectrum of Te_2 at 446 nm. Each data point represents 0.05 cm^{-1}.

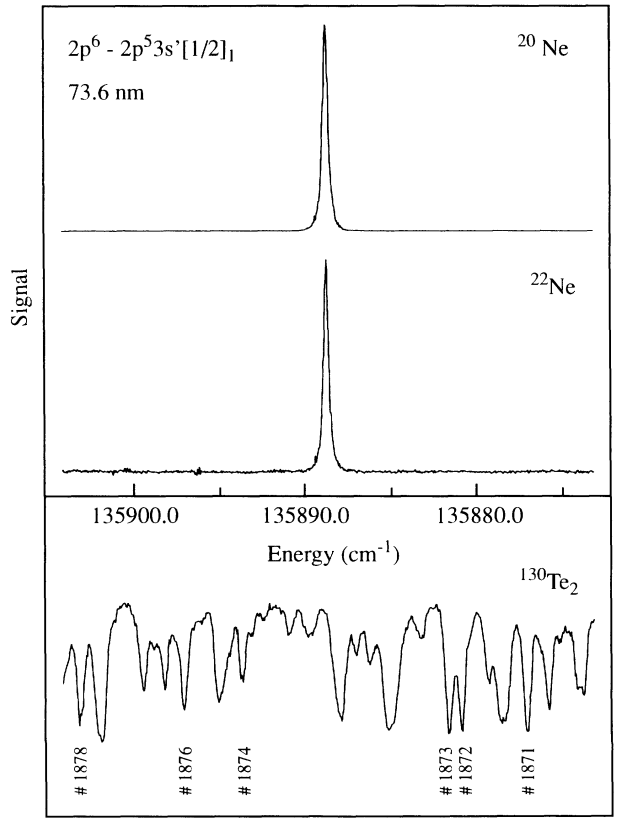

FIG. 4. The $2p^6$-$2p^5 3s'[\frac{1}{2}]_1$ transition in ^{20}Ne and ^{22}Ne at 73.6 nm with the calibration spectrum of Te_2 at 442 nm. Each data point represents 0.05 cm^{-1}.

Minnhagen [21]. The signal-to-noise ratio was about 1000 for ^{20}Ne and 100 for ^{22}Ne (the middle part of Figs. 3 and 4). The 13-times-larger transition probability to $3s'[\frac{1}{2}]_1$ compared to $3s[\frac{3}{2}]_1$ (Chan *et al.* [19]) compensates for the lower xuv yield at the $3s'$ wavelength [Fig. 2(a)]. The linewidth is 0.32(3) cm^{-1}. From the differences between a least-squares linear fit and a spline interpolation between the Te_2 reference lines (the lower part of Figs. 3 and 4), we estimate the absolute uncertainty in the Ne transitions due to nonlinear scanning to be 0.05 cm^{-1}. The statistical error in both transition frequencies was 0.006 cm^{-1}, based on six recordings each. The absolute accuracy of the Te_2 lines [19] results in a 0.01-cm^{-1} error in the xuv frequency. Possible systematic error sources, such as a Doppler shift, contribute less than 0.01 cm^{-1}. Combining all those unrelated errors, an absolute accuracy in the xuv frequency of 0.05 cm^{-1} is deduced.

The isotope shift (^{20}Ne-^{22}Ne) in the $2p^6$-$2p^5 3s'[\frac{1}{2}]_1$ transition is +0.003(3) cm^{-1} and that in the $2p^6$-$2p^5 3s[\frac{3}{2}]_1$ transition, −0.014(3) cm^{-1}. Figure 5 shows a typical isotope-shift recording of both transitions. The high relative accuracy of $\frac{1}{100}$th of the linewidth is possible because of the simultaneous recording of ^{20}Ne and ^{22}Ne, the small isotope shift, and the high signal-to-noise ratio. Under these circumstances, both isotopes experience the same Ne density in the gas pulse and equal fluctuations in xuv frequency and intensity. As a result, ~65% of the noise amplitude is correlated, as far as the dominant features are concerned. The small shift also prevents electron-multiplier saturation on the strong ^{20}Ne signal from distorting the line profiles for ^{22}Ne, which would introduce a systematic error. Extensive computer simulations show that, under these conditions, an error of <0.0025 cm^{-1} is feasible for both transitions. This is in good agreement with the statistical error of <0.003 cm^{-1} in the isotope shift, based on three high- (xuv step size 10^{-2} cm^{-1}) and six low-resolution (xuv step size 5×10^{-2} cm^{-1}) scans. The scan nonlinearity of ~2–3% results in a negligible additional error of <0.0003 cm^{-1}.

The experimental results cannot directly be compared with the many-body calculations of the SMS of the ground state by Veseth [3] as the measured shift involves the effects of both the ground state and the excited level. In Fig. 6 the contributions to the shift of both the $2p^6$ and $2p^5 3s[\frac{3}{2}]_1$ level are shown. The $3s'[\frac{1}{2}]_1$ and $3s[\frac{3}{2}]_1$ level shifts of −0.119(4) and −0.102(4) cm^{-1} are taken from the data of Ritchl and Schober [9,10] extended with the more precise measurements of Odintsov [11]. The accuracy in the excited-state level shifts is mainly determined by the accuracy of 0.003 cm^{-1} stated by Ritchl and Schober. We also compared their transition shifts with the isotope-shift measurements in two-photon transitions from the $3s[\frac{3}{2}]_2$ metastable level by Giacobino, Biriaben, and de Clercq [1]. Combining all these data, an error of 0.004 cm^{-1} in the $3s$ and $3s'$ level shifts can be estimated. The total difference in the mass shift of $2p^6$-$2p^5 3s'[\frac{1}{2}]_1$ and $2p^6$-$2p^5 3s[\frac{3}{2}]_1$ is 0.017(5) cm^{-1}, in excellent agreement with the value of 0.0171(2) cm^{-1} found by Odintsov [10]. Since the same values of Odinstov are used to extract the absolute $3s$ and $3s'$ level shifts, an equal ground-state SMS will result. For this reason, the SMS is evaluated only for the $2p^6$-$2p^5 3s[\frac{3}{2}]_1$ transition.

The NMS is defined as [22]

$$\Delta E = m\frac{(M_H - M_L)}{M_L(M_H + m)}E_L \ .$$

Here, M_L and M_H are the masses of the light and heavy isotopes, respectively; m is the electron mass; and E_L is the level energy for the light isotope. Evaluation of this expression using the nuclear masses by Wapstra and Bos [23] and the ionization energy of Kaufman and Minnhagen [21] results in a ground-state NMS of −13.01 GHz. In combination with the experimental

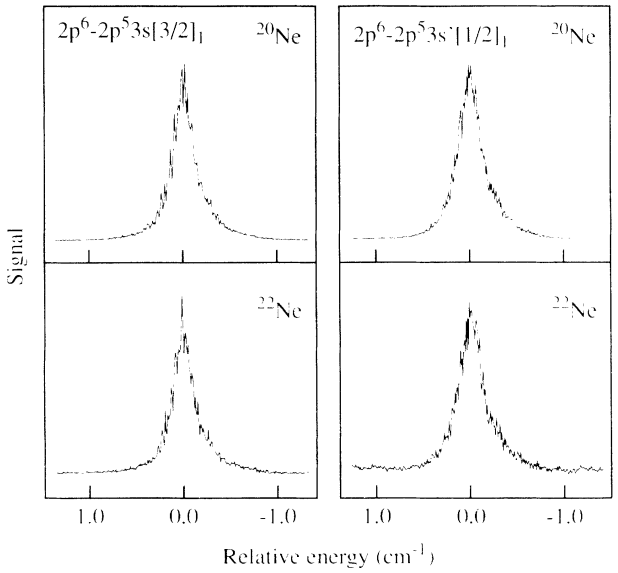

FIG. 5. High-resolution isotope-shift measurement (^{20}Ne-^{22}Ne) of the $2p^6$-$2p^5 3s[\frac{3}{2}]_1$ and $2p^6$-$2p^5 3s'[\frac{1}{2}]_1$ transitions. Each data point represents 0.01 cm^{-1}.

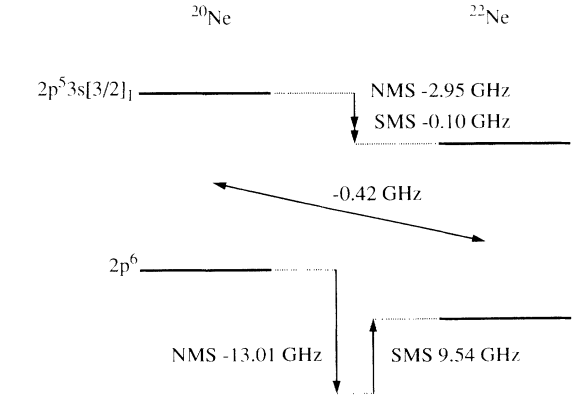

FIG. 6. Schematic of the isotope-shift contributions in the $2p^6$ ground state and the $2p^5 3s[\frac{3}{2}]_1$ excited state [8–10]. The diagonal indicates the measured transition isotope shift (^{20}Ne-^{22}Ne).

TABLE I. Specific mass shift (GHz) of the ground state of neon (^{20}Ne-^{22}Ne). The theoretical values are given for the two different Hamiltonians used in the many-body perturbation analysis of Veseth [3].

	Theory, Ref. [3]		Experiment	
Order	Epstein-Nesbet	Möller-Plesset	Ref. [13]	This work
First	15.00	15.00		
Second	9.46	11.36		
Third	10.05	10.17	11(3)	9.54(15)

values of the level and transition shifts, a SMS of 9.54(15) GHz for the ground state may be deduced. This value is 20 times more accurate than the value of Westerveld and van Eck [13]. It is in good agreement with the theoretical SMS value of ~ 10.1 GHz calculated by Veseth [3], for which, however, no error margin is available. The convergence rate of the Möller-Plesset Hamiltonian used by Veseth suggests an uncertainty of ~ 0.5 GHz (see Table I). However, Veseth points out that the largest error is expected from nonperfect wave functions [3]. Hörbäck *et al.* [7] also used many-body perturbation theory to arrive at a SMS value of 7 GHz, which significantly differs from our experimental value. This discrepancy is probably due to the slow convergence rate of their perturbation analysis [3], in which the effects of the removal of a $2p$ electron from the $2p^6$ closed shell is calculated to second order.

IV. CONCLUSIONS

We have demonstrated that narrow-band xuv radiation produced by third-harmonic generation can be applied for high-resolution spectroscopy. Although two-photon resonances in Xe enhance xuv generation, it is apparent from the measurement of the $2p^6$-$2p^5 3s'[\frac{1}{2}]_1$ transition in neon that is by no means a necessary condition to produce sufficient xuv power for spectroscopy. Furthermore, in the present case the generation of xuv radiation by frequency tripling of uv laser light allows for a direct and simple calibration using the Te_2 absorption spectrum. The measured absolute transition frequencies in neon turn out to be in good agreement with the results of Kaufman and Minnhagen [21]. The measured ground-state SMS is in good agreement with the theoretical value of Veseth [3].

A new value for the ionization energy of ^{20}Ne was derived by Harth, Raab, and Hotop [24] using the $2p^6$-$2p^5 3s[\frac{3}{2}]_2$ transition frequency measured in natural neon by Kaufman and Minnhagen [21]. To obtain the transition frequency for ^{20}Ne, Harth, Raab, and Hotop substracted 0.03 cm^{-1} from this value, based on an estimated transition isotope shift of 0.3 cm^{-1}. However, our measurements, combined with those of Odinstov [10], indicate that this isotope shift is only 0.014(3) cm^{-1} which results in a negligible difference in the $2p^6$-$2p^5 3s[\frac{3}{2}]_2$ transition frequency for natural neon and ^{20}Ne. Therefore, the ionization energy of ^{20}Ne derived by Harth, Raab, and Hotop [24] should be raised by 0.03 cm^{-1}, resulting in a value of 173 929.773(40) cm^{-1}.

Further improvement is feasible using pulsed amplification of cw laser light. Along these lines, it will be possible to reduce the linewidth at least one order of magnitude, allowing for much higher accuracy. However, the limited accuracy of the absolute shifts in the excited state are of major importance in the error budget of the present ground-state SMS. Therefore, any attempt to increase the accuracy in the ground-state SMS value must be accompanied by a recalibration of the absolute shifts in the excited states.

Note added in proof. Through a private communication with Dr. P. Luc we became aware of a calibration shift in the tellurium atlas of 0.002 cm^{-1} based on measurements of Gillaspy and Sansonetti [25]. This results in transition frequencies of 134 459.34(5) cm^{-1} for the $2p^6$-$2p^5 3s$ and 135 888.74(5) cm^{-1} for the $2p^6$-$2p^5 3s'$ lines of neon. The recalibration has no effect on the isotope shifts, or any of the conclusions drawn.

ACKNOWLEDGMENTS

We thank Jacques Bouma for his skillful assistance in the construction of the experimental setup and gratefully acknowledge financial support of the Foundation for Fundamental Research on Matter (FOM), which is part of the Netherlands Organization for Advancement of Research (NWO).

[1] E. Giacobino, F. Biriaben, and E. de Clercq, J. Phys. (Paris) **40**, 1139 (1979).
[2] J. P. Vinti, Phys. Rev. **56**, 1120 (1939).
[3] L. Veseth, J. Phys. B **18**, 3463 (1985).
[4] T. van der Veldt, W. Vassen, and W. Hogervorst, Phys. Rev. A **41**, 4099 (1989).
[5] J. Bauche and R. J. Champeau, Adv. At. Mol. Phys. **12**, 39 (1976).
[6] S. Ahmad, J. Phys. B **18**, 3457 (1985).
[7] S. Hörbäck, A. Mårtensson-Pendrill, S. Salomonson, and U. Österberg, Phys. Scr. **28**, 469 (1983).
[8] R. Ritchl and H. Schober, Phys. Z. **38**, 6 (1937).
[9] H. Schober, Phys. Z. **40**, 77 (1939).
[10] V. I. Odintsov, Opt. Spectrosc. **18**, 205 (1965).
[11] E. Konz, T. Kraft, and H. G. Rubahn, Appl. Opt. **31**, 4995 (1992).
[12] M. M. Salour, Phys. Rev. A **17**, 614 (1978).
[13] W. B. Westerveld and J. van Eck, J. Phys. B **12**, 377 (1979).
[14] K. Miyazaki and H. Sakai, J. Phys. B **25**, L83 (1992).
[15] G. Hilber, A. Lago, and R. Wallenstein, J. Opt. Soc. Am. B **4**, 1753 (1987).

[16] R. H. Page, R. J. Larkin, A. H. Kung, Y. R. Shen, and Y. T. Lee, Rev. Sci. Instrum. **58**, 1616 (1987).
[17] A. Balakrishnan, V. Smith, and B. P. Stoicheff, Phys. Rev. Lett. **68**, 2149 (1992).
[18] K. S. E. Eikema, W. Ubachs, W. Vassen, and W. Hogervorst, Phys. Rev. Lett. **71**, 1690 (1993).
[19] W. F. Chan, G. Cooper, X. Guo, and C. E. Brion, Phys. Rev. A **45**, 1420 (1992).
[20] J. Cariou and P. Luc, *Atlas du Spectre d'Absorption de la Molecule de Tellure* (Laboratoire Aime-Cotton, CNRS II, Orsay, France, 1980), Pt. 5.
[21] V. Kaufman and L. Minnhagen, J. Opt. Soc. Am. **62**, 92 (1972).
[22] W. H. King, *Isotope Shifts in Atomic Spectra* (Plenum, New York, 1984).
[23] A. M. Wapstra and K. Bos, At. Data Nucl. Data Tables **17**, 177 (1977).
[24] K. Harth, M. Raab, and H. Hotop, Z. Phys. D **7**, 213 (1987).
[25] J. D. Gillaspy and C. J. Sansonetti, J. Opt. Soc. Am. B **8**, 2414 (1991).

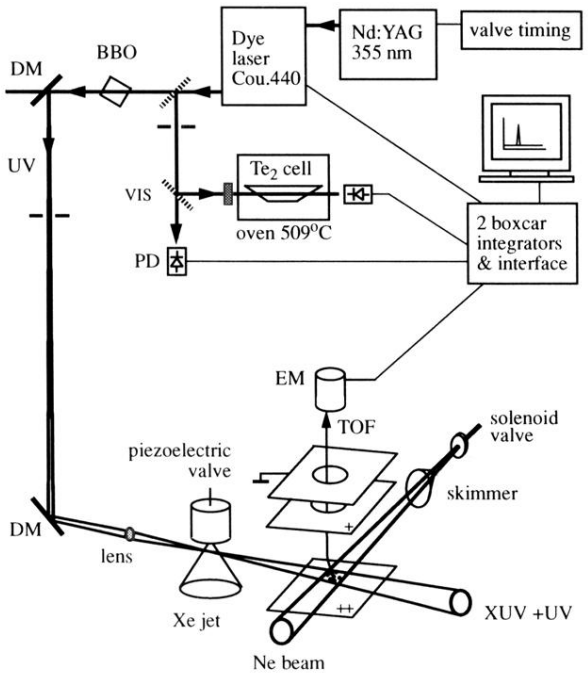

FIG. 1. Schematic of the experimental setup for xuv laser spectroscopy: DM, dichroic mirror; EM, electron multiplier; TOF, time of flight; VIS, visible light; PD, photodiode; and BBO, β-barium borate crystal.